

Uterine lumen fluid is metabolically semi-autonomous

Constantine A. Simintiras ¹, Jessica N. Drum ¹, Hongyu Liu¹, M. Sofia Ortega¹ & Thomas E. Spencer ^{1,2}✉

Uterine lumen fluid (ULF) is central to successful pregnancy establishment and maintenance, and impacts offspring wellbeing into adulthood. The current dogma is that ULF composition is primarily governed by endometrial glandular epithelial cell secretions and influenced by progesterone. To investigate the hypothesis that ULF is metabolically semi-autonomous, ULF was obtained from cyclic heifers, and aliquots incubated for various durations prior to analysis by untargeted semi-quantitative metabolomic profiling. Metabolite flux was observed in these ULF isolates, supporting the idea that the biochemical makeup of ULF is semi-autonomously dynamic due to enzyme activities. Subsequent integrative analyses of these, and existing, data predict the specific reactions underpinning this phenomenon. These findings enhance our understanding of the mechanisms leading to pregnancy establishment, with implications for improving fertility and pregnancy outcomes in domestic animals as well as women.

¹Division of Animal Science, University of Missouri, Columbia, MO 65211, USA. ²Division of Obstetrics, Gynecology, and Women's Health, University of Missouri, Columbia, MO 65201, USA. ✉email: spencerte@missouri.edu

Infertility affects 10–15% of couples¹ with approximately 14% of confirmed pregnancies lost within the first 8 weeks²; however, our understanding of pregnancy establishment remains poor as ~38% of female-factor subfertility is diagnosed as unexplained in women³. The inadequate endometrial function is presumed etiologic for two-thirds of implantation failures⁴. In addition to pregnancy loss, perturbations in the uterine environment can result in chronic adult-onset health impairments for the offspring, in line with the developmental origins of the health and disease paradigm⁵. Female subfertility is also prevalent in cattle, with calving rates often below 30% in dairy cows⁶. Also, most unsuccessful pregnancies fail within the first 21 days post-insemination⁷—the etiology of many of which is a uterine defect, as opposed to paternal or embryo (e.g., aneuploidy) causes⁸. Of relevance, the epithelial lining of the uterine endometrium, particularly the glands, secretes and selectively transports a variety of substances into the lumen of the uterus that is essential for pregnancy establishment via effects on embryo survival, growth, and implantation⁹. Consequently, a better understanding of uterine lumen fluid (ULF) formation and composition regulation is essential to improving fertility and the well-being of subsequent generations.

Conceptus (embryo and extra-embryonic tissues) elongation in ruminants is unique and coincides with a period of high pregnancy loss⁷. The process is characterized by: (i) a morphological transition from spherical to ovoid to tubular to filamentous; (ii) a rapid increase in trophectoderm length, involving cell proliferation that is essential for sufficient production of the maternal pregnancy recognition signal, interferon tau¹⁰; and (iii) onset of extraembryonic membrane differentiation^{11–13}. In cattle, elongation commences around Day 12 and continues through Day 16, which is the day of maternal pregnancy recognition¹¹. Metabolism is presumed central to conceptus elongation as (i) many genes expressed by the elongating conceptus pertain to metabolism^{14,15}; (ii) greater enrichment of differentially expressed genes relating to metabolism was observed in long vs. short (i.e., developmentally incompetent) conceptuses^{16,17}; (iii) progesterone (P4) acts via the endometrium to amplify select endometrial metabolites in ULF by Day 14¹⁸; and (iv) metabolically related enzymes dominate proteins in the ULF by Day 15. Indeed, the largest protein function categories of the Day 16 ULF proteome are “metabolic processes” and “catalytic activity”¹⁹.

Bovine^{18–20} and human²¹ ULF are highly dynamic and contain metabolically relevant enzymes. Accordingly, our central hypothesis is that ULF is metabolically semi-autonomous, i.e. that select biochemical pathways are active within ULF due to enzymatic activity and occur independently of external influences²². This phenomenon has been observed in cerebrospinal fluid (CSF)—an interstitial fluid, like ULF—in which the tryptophan–kynurenine pathway is active²³. Furthermore, imbalances in CSF tryptophan, kynurenine, kynurenic acid, and quinolinic acid levels are associated with neurodegenerative disorders, such as multiple sclerosis, schizophrenia, and Alzheimer’s disease²³. As such, it is tempting to suggest that the metabolic semi-autonomy of CSF may be a physiologically relevant phenomenon.

To test whether ULF is also metabolically semi-autonomous, ULF from cattle was sampled, aliquoted, and incubated for various durations, prior to comprehensive metabolomic analysis. The resulting data support the hypothesis that ULF is metabolically semi-autonomous. Moreover, the semi-autonomous reactions in the ULF involve metabolites associated with conceptus development, as well as metabolites previously identified in the ULF of highly fertile animals—cumulatively suggestive of this phenomenon being physiologically significant.

Results and discussion

To test our hypothesis that ULF is metabolically semi-autonomous, the estrous cycles of nine dairy heifers were synchronized, and ULF was sampled using a non-surgical approach on Days 12 and 16 by uterine lavage using phosphate-buffered saline (PBS) (Fig. 1a). The recovered ULF was immediately aliquoted, incubated for various durations, and then comprehensively analyzed by high-throughput untargeted semi-quantitative metabolomics (Fig. 1b). Cyclic (non-pregnant) animals were selected as the conceptus secretes many metabolites¹³ and enzymes²⁴. Thus, sampling ULF from cyclic animals allowed us to interrogate our hypothesis in ULF free from compounding conceptus-derived factors.

Mean (\pm S.D.) serum P4 at the time of ULF lavage of Day 12 and 16 cohorts was $6.5 \pm 1.9 \text{ ng ml}^{-1}$ and $8.9 \pm 2.3 \text{ ng ml}^{-1}$, respectively (Fig. 1c); correspondingly, mean (\pm S.D.) *corpus luteum* diameters were $22.6 \pm 2.7 \text{ mm}$ (Day 12) and $20.5 \pm 1.9 \text{ mm}$ (Day 16), cumulatively confirming successful estrous cycle synchronization. Moreover, total protein was measured in control ULF aliquots (Fig. 1b), and the mean (\pm S.D.) across all heifers was $2.0 \pm 1.6 \mu\text{g ml}^{-1}$ (Fig. 1d). As the total volume of fluid in the uterine lumen is approximated to be $200 \mu\text{l}$ in cattle²⁵—and extrapolating that the 10 ml PBS flush conducted here resulted in a 50-fold dilution—we can assume that the ULF retrieved here, undiluted, comprised $100 \mu\text{g ml}^{-1}$ protein. For reference, single mammalian cells contain about $200 \mu\text{g ml}^{-1}$ protein²⁶. Thus, the total protein concentration of ULF observed is orders of magnitude lower than what would be expected from mass cell lysis. Further, the total concentration of all metabolites in the ULF of each heifer on Days 12 (Fig. 1e) and 16 (Fig. 1f) remained unchanged during incubation, further confirming that any exogenous metabolite consumption or release was negligible at worst, and absent at best.

A total of 317 metabolites were detected in ULF on Day 12, with just 7 additional metabolites identified on Day 16 (Fig. 2a), despite 134 (Fig. 2b) vs. 230 (Fig. 2c) metabolites common to the ULF of all subjects on each respective day. The majority of these 317 metabolites clustered under lipid and amino acid metabolism (Fig. 2d), similarly to ULF from beef heifers on Days 12–14¹⁸. Regarding the hypothesis, metabolite flux was observed in ULF on Days 12 (Fig. 2e) and 16 (Fig. 2f), confirming that the biochemical makeup of ULF is indeed semi-autonomously dynamic. In fact, observed individual metabolite flux increases include: 15.5-fold (diethanolamine); 13.2-fold (N-palmitoyl-sphingosine); 9.8-fold (spermine); 9.6-fold (mannitol/sorbitol); and 7.4-fold (butyrylcarnitine) (Supplementary Data 1). Specific examples of multi-directional individual metabolite levels over time are presented in Fig. 2g–t.

Interestingly, individual metabolite concentrations (Fig. 2u), as well as flux (Fig. 2e, f), were relatively inconsistent across subjects, as cumulatively summarized by Fig. 2v. Specific examples include 3-hydroxy-3-methylglutarate—which displayed an increasing trend in the ULF lavage of one subject on Day 12 (Fig. 2g), yet the opposite trajectory in a different Day 12 subject (Fig. 2h). Similarly, putrescine levels rose in a Day 16 ULF lavage (Fig. 2q) and fell during the incubation of another lavage from a different Day 16 subject (Fig. 2r).

Two inevitable aetiologies likely underly this heterogeneity: (i) biological variation between animals (inter-subject variation; Fig. 2u); and (ii) asynchrony (intra-subject variation). The latter may be partially reflected by serum P4 level variation (Fig. 1c). It is worth noting that achieving perfect estrous cycle synchrony is impossible²⁷—in other words, we suspect that, had we lavaged these uteri just 5 min sooner or later, the trends presented in Fig. 2g–t may look quite different. Nonetheless, despite this inevitable heterogeneity, these data demonstrate that ULF is, in

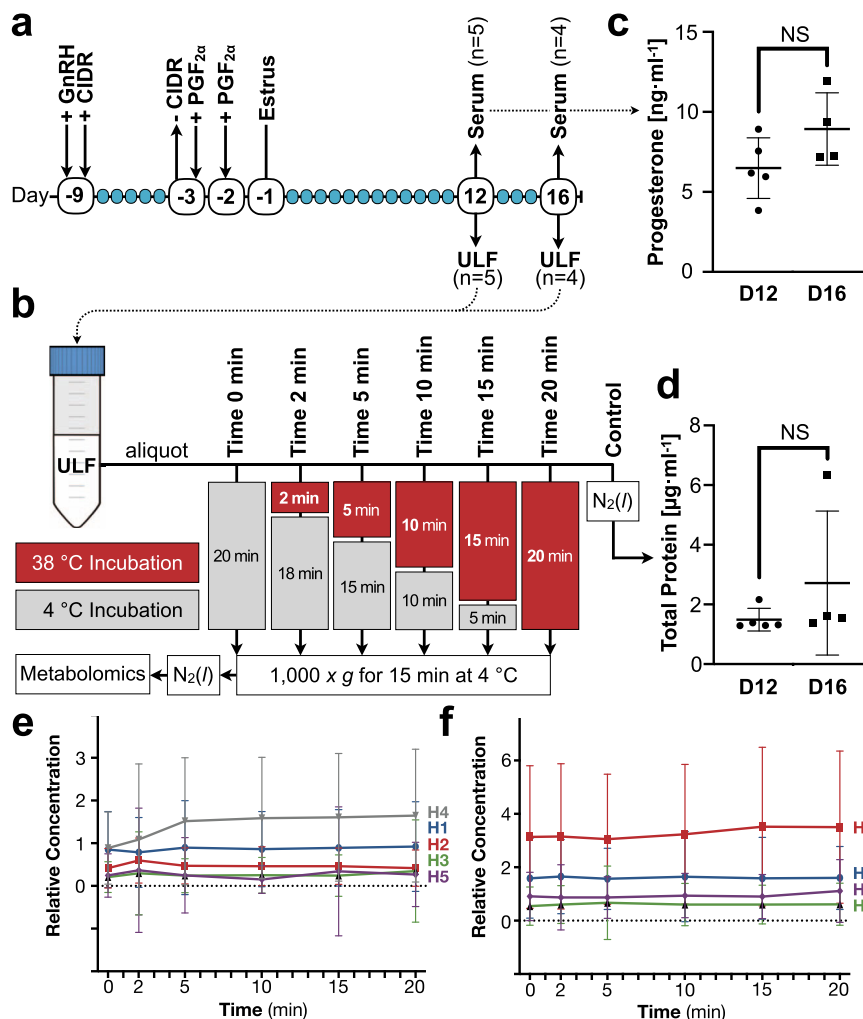


Fig. 1 Experimental design depiction and validation. **a** The estrous cycles of nine heifers (H) were synchronized by administration of: gonadotropin-releasing hormone (GnRH); controlled internal drug release (CIDR) intra-vaginal progesterone insert; and prostaglandin F_{2α}. Uterine lumen fluid (ULF), and serum, were recovered on Days 12 and 16. **b** Recovered ULF was aliquoted and select aliquots were incubated for various durations prior to centrifugation and supernatant storage until analysis. **c** Mean (horizontal line \pm S.D.) serum progesterone levels of heifers from which ULF was obtained, at the time of isolation, on Day 12 (D12; H1-5; $n = 5$) or 16 (D16; H1-4; $n = 4$). **d** Mean (horizontal line \pm S.D.) total protein concentration of control ULF lavage aliquots on D12 ($n = 5$) and D16 ($n = 4$). **e, f** Mean (\pm S.E.M.) relative concentration of all ULF metabolites on D12 ($n = 317$); **e** and D16 ($n = 324$); **f** from each heifer throughout the ULF incubation period. No effect of time or heifer was observed. Additional abbreviations: not significant (NS).

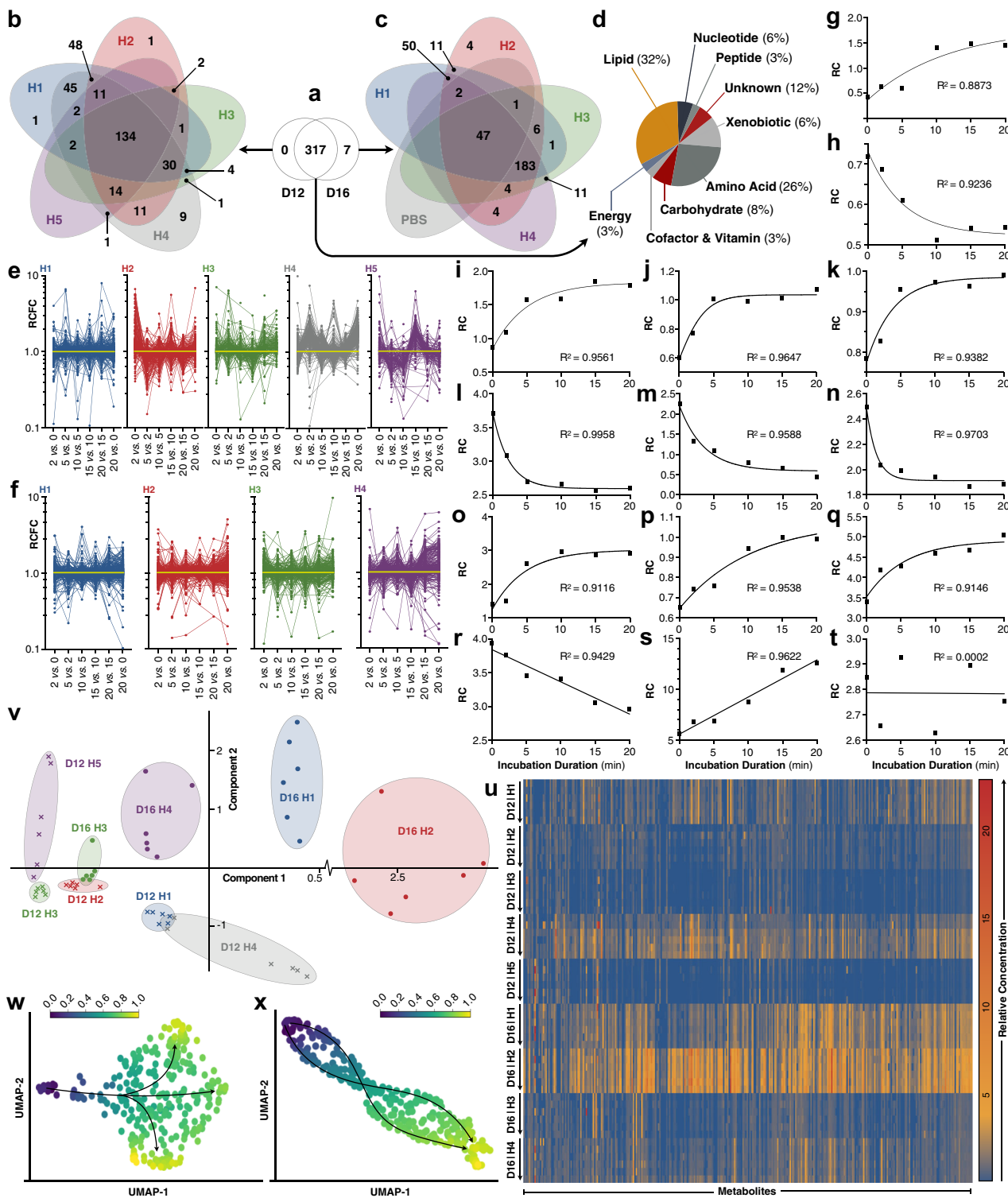
fact, a semi-independently dynamic microenvironment, and, therefore, metabolically semi-autonomous, as hypothesized.

To identify potential commonalities among these data, bioinformatic pseudotime analyses were performed. More specifically, given that single uterine lavages were obtained from each subject, these metabolomic data are inherently cross-sectional, thus lacking biological temporal specificity and resolution. Thus, to partially circumvent this, trajectorial inference, or pseudotime, analyses, were performed to map this high-dimensional, cross-sectional, and asynchronous data (Supplementary Data 1 and 2) to a series of one-dimensional quantities (pseudotimes), for measuring any relative progression in the absence of explicit time series data²⁸. The results suggest that three divergent pathways exist in the ULF of Day 12 subjects (Fig. 2w), compared to two, seemingly functionally redundant, pathways on Day 16 (Fig. 2x).

Thereafter, to probe the specific metabolites underpinning these findings across all subjects, we analyzed the data *en masse* and identified 33 metabolites exhibiting ($P \leq 0.05$) or trending ($0.05 < P \leq 0.10$) towards exhibiting significant flux by day (Fig. 3). More specifically—despite the aforementioned

inter-subject ULF variation, some overlap was observed, as—the concentrations of 4 metabolites differed, and 10 trended towards a difference during the incubation of ULF collected on Day 12 ($n = 5$). Correspondingly, the levels of 13 metabolites differed, and 8 trended towards differing during the incubation of ULF on Day 16 ($n = 4$). In other words, these differences were statistically uniform across all heifers on each given day. Thus, different metabolic pathways appear active in ULF on Day 12 (expected day of conceptus elongation onset) as compared to Day 16 (expected day of maternal pregnancy recognition), as previously suggested by pseudotime analysis. Interestingly, regarding the statistically significant directionality of this metabolite flux, some trajectories were uniform [e.g., 3-methylcytidine; (iso)butyrate; nicotinamide riboside; and spermine], whereas others fluctuated (e.g., glutarate; methylsuccinate; and ophthalmate). In the future, reducing ULF incubation intervals while increasing the overall incubation duration may shed light on broader metabolite flux trends at play.

Next, to piece together the precise reactions underpinning the observed metabolic semi-autonomy of ULF, these data were



cross-referenced against prior interrogations of the ULF proteome. Thereafter, to probe whether this predicted mechanism of ULF metabolic semi-autonomy may have physiological relevance (i.e., contribute to maternal-embryo dialogue), we conducted an integrative analysis, incorporating previous ULF metabolomic, as well as conceptus-conditioned media proteomic and metabolomic, data, as cumulatively presented in Fig. 4a and described below.

Moraes et al. previously probed the proteome and primary metabolome of ULF from embryo-transferred fertility-classed

heifers on Day 17, and the ULF was obtained by flushing the uterus post-mortem²⁰. Levels of 221 proteins differed in high (HF) vs. low (LF) fertility cattle—namely revolving around amino acid synthesis, vitamin B6 metabolism, and energy metabolism. Similarly, 70 (of 122 identified) metabolites differed in the ULF of HF vs. LF heifers. Interestingly, of the top 20 differentially abundant metabolites in HF vs. LF subjects, 30% correspond to metabolites and pathways predicted central to the semi-autonomous metabolic cascades of ULF (Fig. 4a). Another study examining the ULF metabolome on Days 12 and

Fig. 2 Uterine lumen fluid is metabolically semi-autonomous. **a** Venn diagram of the number of metabolites present in the uterine lumen fluid (ULF) of heifers on Day 12 (D12) vs. 16 (D16). **b, c** Breakdown of the number of metabolites identified, or not, in the ULF of each heifer (H) on **b** Day 12 (H1–5), and **c** Day 16 (H1–4), in addition to the phosphate-buffered saline (PBS) lavage control. **d** Super-pathway distribution of the metabolites identified in ULF on both days ($n = 317$). **e, f** Relative concentration fold-changes (RCFC) of all individual metabolites in Day 12 (**e**) and Day 16 (**f**) ULF of each heifer (H1–H5) between incubation intervals. **g–t** Examples of specific individual metabolite flux [relative concentrations (RC)] over time within single uteri, with corresponding trendlines and coefficients of determination (R^2). Specifically: **g** 3-hydroxy-3-methylglutarate (D12/H3); **h** 3-hydroxy-3-methylglutarate (D12/H2); **i** 5-oxoproline (D12/H3); **j** fructose (D12/H4); **k** glycerophosphocholine (D12/H1); **l** nicotinamide mononucleotide (D12/H1); **m** spermidine (D12/H1); **n** phenylacetyl glycine (D12/H1); **o** arginine (D16/H4); **p** sphingosine (D16/H1); **q** putrescine (D16/H1); **r** putrescine (D16/H2); **s** urate (D16/H2); and **t** N-acetyl glycine (D12/H1). **u** Heatmap of individual metabolite relative concentration variation across heifers. Arrows correspond to incubation timepoints in ascending order. Shades of blue, yellow, and red correspond to metabolite relative concentrations, whereas green cells denote undetected metabolites. **v** Landmark Principal Component Analysis of ULF from all heifers. Each point represents the metabolomic profile of ULF at a single incubation time-point. **w, x** Pseudo-time analysis of the **w** Day 12 and **x** Day 16 ULF metabolome from all heifers at all incubation intervals. Additional abbreviation: uniform manifold approximation and projection unit (UMAP).

14 from heifers with high systemic P4—a model of accelerated conceptus elongation—found 19 elevated metabolites in the ULF of high vs. normal P4 heifers¹⁸, of which 21% are common to the model of ULF semi-autonomy presented here (Fig. 4a). Moreover, an intimate relationship between conceptus-secreted metabolites¹³ and enzymes²⁴ and the ULF metabolome data generated here is apparent (Fig. 4a), further supporting the idea that the metabolic semi-autonomy of ULF plays a role in uterine support of conceptus elongation and pregnancy establishment. Specific biochemical players, central to this phenomenon and previously identified as being of potential reproductive significance include glutarate, myo-inositol, sorbitol, spermidine, and spermine. Figure 4b highlights select biochemical reactions predicted to be similarly semi-autonomous in human ULF, based on published proteomic analyses²¹.

Regarding study limitations, retrieving ULF using smaller lavage volumes prior to analysis may improve both metabolomic analytical sensitivity and enzymatic proximity, to yield a higher-resolution atlas of active reactions. However, there is, unfortunately, no perfectly clean way to retrieve ULF. Here, we opted for direct retrieval by lavage, as opposed to in situ cannulation or *post-mortem* excision and flushing, as it presents a lower risk of sample deviation from the in vivo environment²⁹. Cannulation of the uterine lumen would cause local inflammation and contamination. Spontaneous metabolite thermal degradation could also skew the data, particularly as metabolites in this study were underivatized. However, we do not expect this to be significant as glutamate, a notoriously unstable metabolite³⁰ remains intact in solution for over 60 min at 60 °C³¹. The longest incubation duration in the present study was 20 min at 38 °C. Residual cellular, a cellular organelle, or blood contamination in the ULF was minimized in the present study as (a) visibly blood-contaminated ULF flushes were not utilized in this study (see Methods); (b) ULF aliquots were incubated in a closed system (Fig. 1e, f); and (c) low protein levels were present in all samples included for analysis (Fig. 1d).

Future work includes (a) similarly confirming the existence of this phenomenon in women, as predicted (Fig. 4b), and (b) interrogating the hypothesis that the degree of metabolic autonomy of ULF is linked to fertility. The latter could be used to develop biomarkers of fertility, and interventions to restore inadequate endometrial function. In closing, these data show that ULF biochemistry is semi-autonomously dynamic. Using cattle as a model, we demonstrate that select biochemical pathways are active within ULF, due to enzymatic activity. This finding, within the context of existing literature, enhances our understanding of the biochemical mechanisms leading to pregnancy establishment, with implications for improving fertility in domestic animals and women.

Methods

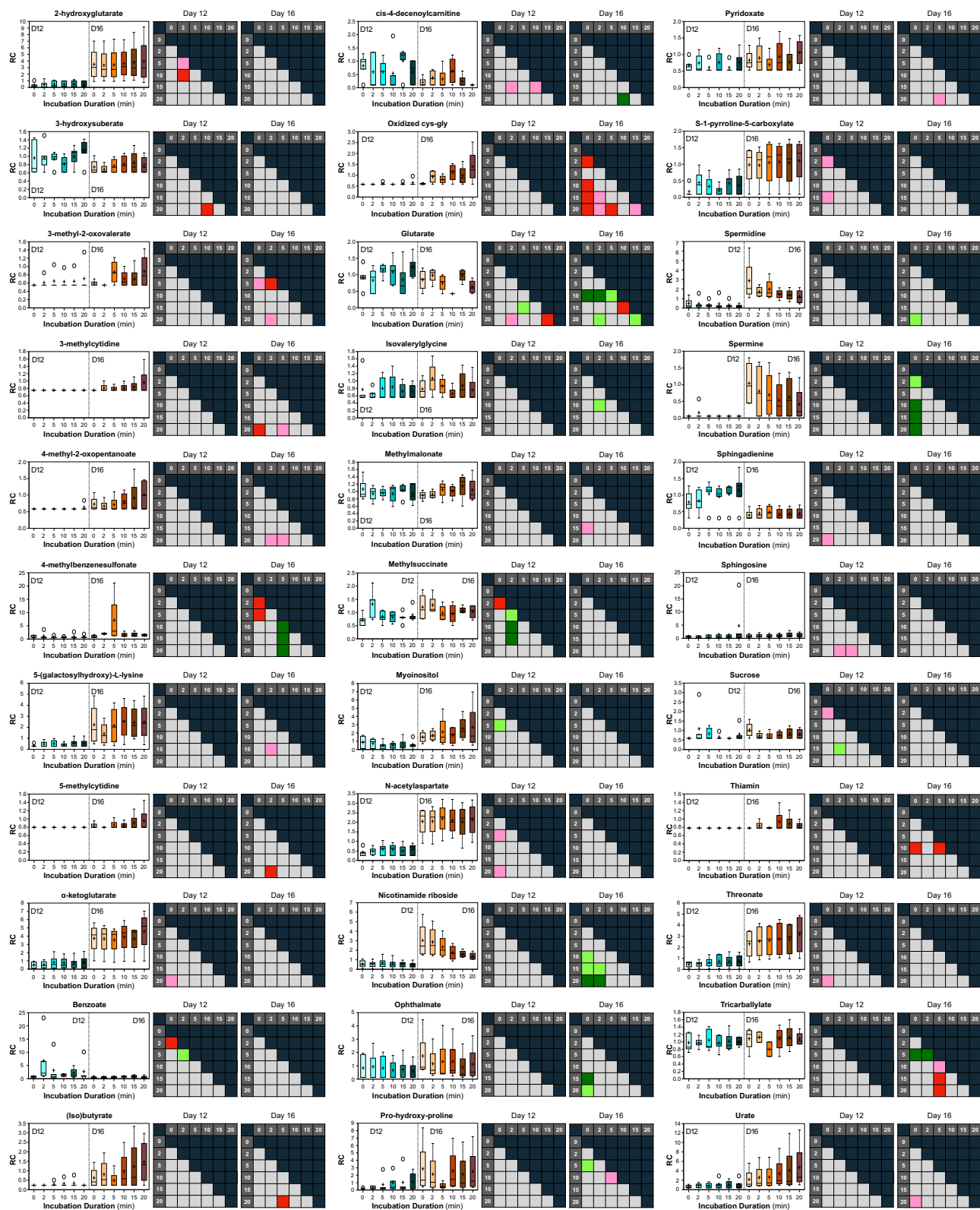
Animals. All animal procedures were conducted in accordance with the Guide for the Care and Use of Agriculture Animals in Research and Teaching and approved by the Institutional Animal Care and Use Committee at the University of Missouri. Fifteen (15) Holstein heifers were used averaging 15 months of age with a mean (\pm S.D.) body condition score (scale of 1–5) of 3.04 ± 0.44 and 766.6 ± 62.8 kg weight. On a random day of their estrous cycle, heifers were synchronized to estrus using an established protocol³². As depicted in Fig. 1a, heifers initially received a dose of gonadotropin-releasing hormone, coupled to the insertion of a controlled internal drug release (CIDR) intravaginal P4 insert (1.9 g, CIDR, Zoetis, NJ, USA). CIDR removal occurred 6 days thereafter, at which time, a PGF_{2 α} dose (25 mg Dinoprost, Lutalyse, Zoetis, NJ, USA) was also administered, and heat detection patches (Estroject, TN, USA) were applied. A second PGF_{2 α} dose was administered 24 h later and heifers were visually observed for standing estrus at 12 h intervals for 72 h. Estrus was designated by heat detection patch activation.

Thereafter, heifers were distributed in two experimental groups for ULF retrieval on Days 12 and 16 post-estrus (Fig. 1a). On the day of ULF retrieval, the presence of an ovarian *corpus luteum* was confirmed by transrectal ultrasonography prior to uterine lavage³³. Specifically, 10 ml PBS was gently expelled into the uterine body using a silicone catheter coupled to a syringe. The uterine body was gently massaged transrectally, and ULF was recovered by generating a mild negative pressure using the syringe. Upon retrieval, ULF was immediately processed as described below. All flushes were performed by the same technician. Of the 15 heifers initially enrolled, two were excluded on account of not exhibiting signs of estrus. The remaining 4 were removed, as ULF flushes were visibly contaminated with blood based on color.

Uterine lavage collection and processing. Uterine lavage were immediately equally apportioned into 7 aliquots (Fig. 1b). All but two aliquots from each lavage were incubated at 38 °C with shaking (Genie Temp Shaker 100; Scientific Industries; Bohemia, NY, USA) for either 2, 5, 10, 15, or 20 min. Following incubation, these aliquots were immediately placed at 4 °C to effectively quench enzymatic activity and then clarified by centrifugation at 1000 \times g for 15 min at 4 °C (5424R; Eppendorf, Hamburg, Germany). One aliquot (Time 0) was maintained at 4 °C for 20 min prior to centrifugation as described. The supernatants were submerged in N₂(l) and stored at –80 °C until shipment for analysis on dry ice, as described below. A “control” aliquot (Fig. 1b) was not processed and immediately flash frozen in N₂(l) and stored at –80 °C until total protein was quantified (Fig. 1d) using a Qubit 3.0 Fluorometer (ThermoFisher, Waltham, MA, USA) as per manufacturer instructions.

Progesterone quantification. To measure systemic progesterone (Fig. 1c), blood was withdrawn by coccygeal venipuncture into 10 ml vacutainer tubes (Fisher Scientific, Hampton, NH, USA) after uterine lavage and centrifuged at 1500 \times g for 20 min at 4 °C. The supernatant (serum) was recovered and stored at –80 °C until analysis. Serum progesterone was quantified by double-antibody radio-immunoassay (MP Biomedicals, California, USA)³⁴. The intra-assay coefficient of variation was 4% and assay sensitivity was 0.05 ng ml^{–1}.

Metabolomic profiling. Metabolomic analyses were performed by ultrahigh performance liquid chromatography–tandem mass spectroscopy (UPLC–MS/MS) by Metabolon Inc. (Durham, NC, USA)^{13,18,35}. Briefly, the protein was precipitated and extracted using the automated MicroLab STAR system (Hamilton Company) with methanol under vigorous centrifugation at 680 \times g for 2 min (Geno/Grinder 2000, Glen Mills) prior to methanol removal by TurboVap (Zymark) and overnight incubation in N₂. Each sample was subsequently divided into four fractions—two for analysis by reverse-phase (RP) UPLC–MS/MS with positive ion mode electrospray ionization (ESI), one for analysis by RP UPLC–MS/MS with negative ion mode ESI, and one for analysis by hydrophilic interaction liquid



chromatography (HILIC) UPLC-MS/MS with negative ion mode ESI. Sample extracts were then dried and reconstituted in solvents as outlined below.

The first fraction, analyzed under positive ionization, was subject to gradient elution (Waters UPLC BEH 1.7 μ m C18 column 2.1 \times 100 mm) in water and methanol with 0.05% perfluoropentanoic acid and 0.1% formic acid. The second fraction, run under positive ESI, was identically eluted, using the same column, but with an elution buffer additionally comprising acetonitrile. The third fraction, analyzed under negative ionization, was also eluted by a gradient buffer comprising

methanol, water, and 6.5 mM ammonium bicarbonate (pH 10.8). The last fraction, run under negative ESI, was eluted using a HILIC (Waters UPLC BEH Amide 1.7 μ m column 2.1 \times 150 mm) with a water and acetonitrile plus 10 mM ammonium formate (pH 10.8) gradient.

Samples were analyzed using a Waters Acquity UPLC coupled to a Thermo Scientific Q-Exactive high-resolution MS interfaced with heated electrospray ionization (HES-II) source and Orbitrap mass analyzer operating at 35,000 mass resolution and with a scan range between 70 and 1000 m/z . Metabolites were

Fig. 3 Qualitative and semi-quantitative interrogation of uterine lumen fluid metabolic semi-autonomy. Metabolites exhibiting statistically significant ($P \leq 0.05$), or trending towards significant ($0.05 < P < 0.10$), flux during incubation in Day 12 (D12; $n = 5$) and Day 16 (D16; $n = 4$) uterine lumen fluid (ULF). Predicted and unknown metabolites are excluded. Scaled intensities of select metabolites are provided, wherein the central horizontal line represents the median value with outer boundaries depicting upper and lower quartile limits. Error bars depict the minimum and maximum distributions, with a simple cross representing the mean value and an open circle the extreme data point. Corresponding statistical comparisons are also provided, wherein dark green shading indicates a significant ($P \leq 0.05$) decrease (metabolite ratio < 1.0) between groups, whereas light green depicts a decreasing trend ($0.05 < P < 0.10$). Conversely, dark red shading indicates a significant ($P \leq 0.05$) increase (metabolite ratio > 1.0) between groups, with pink depicting an increasing trend ($0.05 < P < 0.10$). Gray cells indicate the mean fold-change value was not significantly different for that comparison.

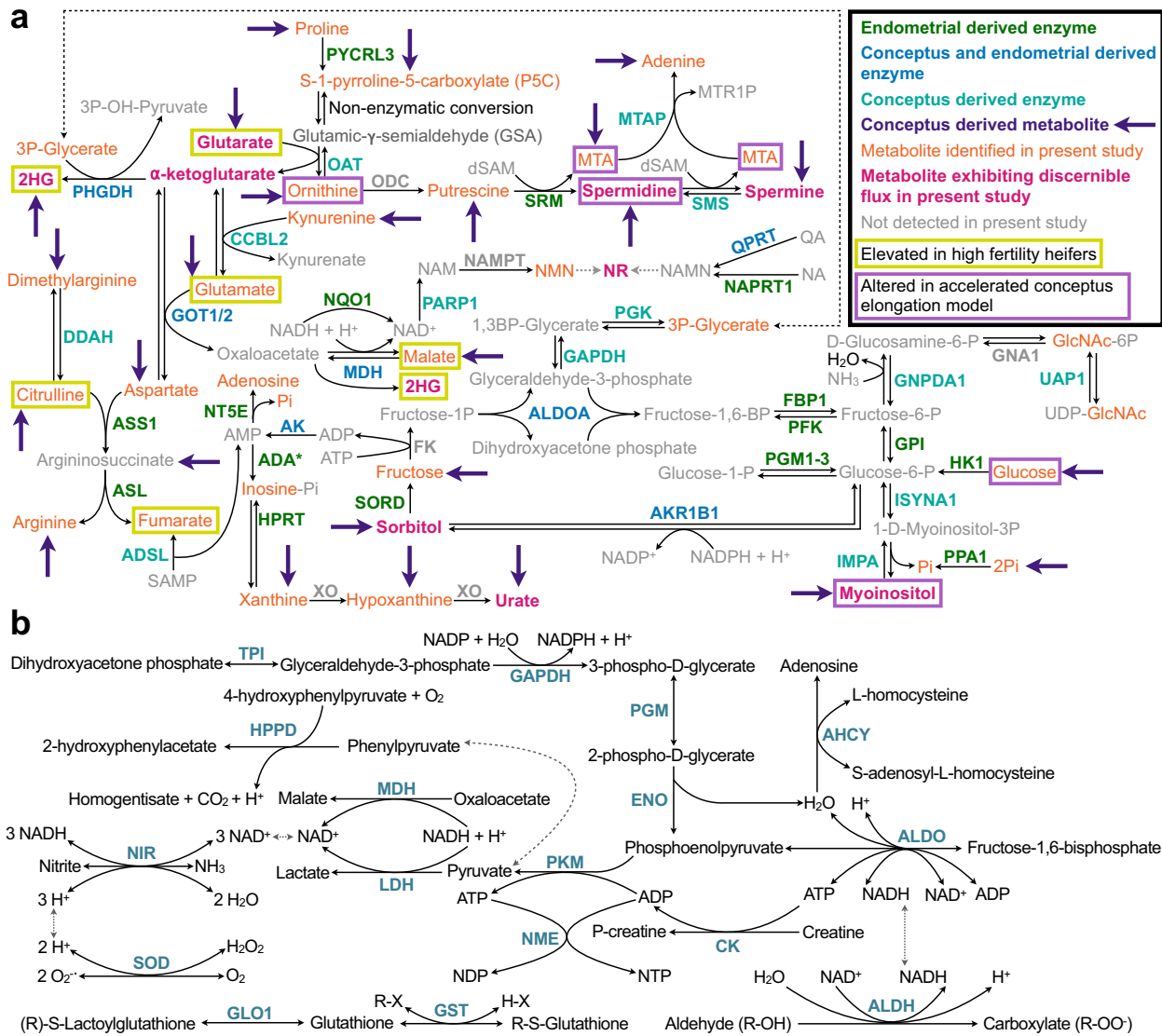


Fig. 4 Predicted mechanism underpinning the metabolic semi-autonomy of uterine lumen fluid. **a** Extrapolated pathways active in bovine uterine lumen fluid (ULF) based on: (i) ULF proteomic data¹⁹; (ii) conceptus conditioned culture medium proteomic²⁴ and metabolomic¹³ data—representing potentially active pathways during pregnancy; (iii) ULF metabolomic data presented in this study; (iv) ULF metabolomics from high vs. low fertility heifers²⁰; and ULF metabolomic profiling from heifers with high systemic P4 (a model of accelerated conceptus elongation)¹⁸. **b** Predicted pathways active in human ULF based on existing proteomic data²¹. Abbreviations: 2-hydroxyglutarate (2HG); 5'-methylthioadenosine (MTA); 5-methylthioribose-1-phosphate (MTR1P); adenosine tri- (ATP), di- (ADP), and mono- (AMP) phosphate; decarboxylated s-adenosyl methionine (dSAM); inorganic phosphate (Pi); N-acetylglucosamine (GlcNAc); nicotinic acid (NA); nicotinic acid mononucleotide (NAMN); nicotinamide mononucleotide (NMN); nicotinamide (NAM); adenine dinucleotide (NAD) phosphate (NADPH); nicotinamide riboside (NR); succinyl-adenosine monophosphate (SAMP); uridine diphosphate (UDP); and quinolinic acid (QA). Enzyme abbreviations are listed in the Human Genome Organization (HUGO) Gene Nomenclature Committee database (genenames.org).

quantified against known internal and recovery standards, run in parallel at random intervals. Identification was based on retention time and an m/z within ± 10 ppm. The technical (instrument) median relative standard deviation was 5% with a total process variability of 10%.

Three controls were analyzed in parallel with the experimental samples: (i) a pooled aliquot of all experimental samples, serving as a technical replicate control; (ii) ultra-pure water samples served as process blanks, also run in between the experimental samples at defined intervals; and (iii) a cocktail of quality control metabolites, absent from endogenous compound measurements, were spiked into each sample. The latter internal standard enabled instrument performance monitoring and chromatographic alignment.

Metabolomic data extraction and analyses. Data were corrected for variations resulting from instrument inter-day tuning differences; median peak areas for each metabolite were registered as 1.00 prior to the proportional normalization and logarithmic transformation of each data point. For qualitative metabolomic analyses (e.g., Fig. 2), these data (Supplementary Data 1) were used (i.e., individual metabolite presence and/or flux, within the ULF of single heifers, were analyzed, with neither imputation nor statistical analysis). For semi-quantitative metabolomic interpretation (e.g., Fig. 3), missing values, if any, were imputed with the minimum observed value for each compound (Supplementary Data 2) prior to quantification by relative abundance using MetaboLync pathway analysis software (portal.metabolon.com), wherein statistical comparisons were made by two-way ANOVA with a $P \leq 0.05$ or $0.05 < P < 0.10$ cut off.

Pseudotime analysis. Pseudotime analysis (Fig. 2w, x) was performed using partition-based graph abstraction, as in Wolf et al.³⁶, to produce uniform manifold approximation and projection for dimension reduction projections in K-nearest neighbors space. More specifically, the Leiden Cluster Determination algorithm was applied to the relative concentration of all metabolites ($n = 324$) at each time point ($n = 6$), from the ULF of all heifers [Day 12 ($n = 5$) and 16 ($n = 4$)]. In summary, 9720 (Day 12) and 7776 (Day 16) data points were condensed to 9 and 10 clusters, respectively. Cluster trajectories (pseudotimes) were visualized by applying the ForceAtlas2 (FA) algorithm.

Integrative metabolomic analyses. To predict the precise reactions underpinning the semi-autonomous metabolic nature of ULF (Fig. 4a), existing published datasets (cited below), in addition to Supplementary Data 1 and 2, were utilized. Specifically, endometrial-derived enzymes in ULF were gleaned from Forde et al.¹⁹, whereas conceptus and endometrial-derived enzymes were determined from Forde et al.²⁴. Enzymes were considered conceptus-derived if present in conceptus-conditioned media²⁴ but not in ULF from cyclic (non-pregnant) heifers¹⁹. Metabolites elevated in the ULF of high-fertility heifers vs. those of low fertility was established by Moraes et al.²⁰, whereas metabolites elevated in the ULF of heifers with high systemic P4 (a model of accelerated conceptus elongation) are presented in Simintiras et al.¹⁸. Conceptus-conditioned media metabolites were identified in Simintiras et al.¹³. Human ULF proteomic data (Fig. 4b) were gleaned from DeSouza et al.²¹.

Statistics and reproducibility. Serum progesterone (Fig. 1c) and ULF protein (Fig. 1e) comparisons were conducted by unpaired t-test using Prism 8 (GraphPad, San Diego, CA, USA). Total metabolite flux data (Fig. 1f-g) were visualized and statistically contrasted by two-way ANOVA coupled to Tukey's non-parametric post hoc using Prism 8. Semi-quantitative individual metabolite flux (Supplementary Data 1) visualizations per subject (Fig. 2e-f) and per metabolite (Fig. 2g-t) were also achieved using Prism 8, as was heatmap (Fig. 2u) generation. Principal component analysis (Fig. 2v) was performed using the open-access Past4 software³⁷. To elucidate common trends in metabolite flux, metabolomic data (Supplementary Data 2) were compared by two-way ANOVA, with $P \leq 0.05$ denoting significance and $0.05 < P < 0.10$ highlighting a trend toward significance. Metabolite flux was determined when a significant or trending difference was observed in ≥ 1 time-course comparison within a corresponding day (Supplementary Data 2; Fig. 3). All measurements were taken from distinct samples.

Reporting summary. Further information on research design is available in the Nature Research Reporting Summary linked to this article.

Data availability

All data used to generate figures are provided with this paper and/or associated supplementary material. The raw metabolomic data are deposited in Dryad (datadryad.org) under Simintiras et al.³⁸. Any additional information may be available from the corresponding author upon reasonable request.

Code availability

The code used for pseudotime analysis is available on GitHub via <https://bit.ly/3JpaLXD>.

Received: 21 July 2021; Accepted: 8 February 2022;

Published online: 01 March 2022

References

- Evers, J. L. H. Female subfertility. *Lancet* **360**, 151–159 (2002).
- Rossen, L. M., Ahrens, K. A. & Branam, A. M. Trends in risk of pregnancy loss among US women, 1990–2011. *Paediatr. Perinat. Epidemiol.* **32**, 19–29 (2018).
- Hull, M. G. et al. Population study of causes, treatment, and outcome of infertility. *Br. Med. J.* **291**, 1693–1697 (1985).
- Edwards, R. G. Implantation, interception and contraception. *Hum. Reprod.* **9**, 985–995 (1994).
- Barker, D. J. The fetal and infant origins of adult disease. *Br. Med. J.* **301** 1111 (1990).
- Sartori, R., Bastos, M. R. & Wiltbank, M. C. Factors affecting fertilisation and early embryo quality in single- and superovulated dairy cattle. *Reprod. Fertil. Dev.* **22**, 151–158 (2010).
- Walsh, S. W., Williams, E. J. & Evans, A. C. O. A review of the causes of poor fertility in high milk producing dairy cows. *Anim. Reprod. Sci.* **123**, 127–138 (2011).
- Wiltbank, M. C. et al. Pivotal periods for pregnancy loss during the first trimester of gestation in lactating dairy cows. *Theriogenology* **86**, 239–253 (2016).
- Kelleher, A. M., Demayo, F. J. & Spencer, T. E. Uterine glands: developmental biology and functional roles in pregnancy. *Endocr. Rev.* **40**, 1424–1445 (2019).
- Bazer, F. W. & Thatcher, W. W. Chronicling the discovery of interferon tau. *Reproduction* **154**, F11–F20 (2017).
- Brooks, K., Burns, G. & Spencer, T. E. Conceptus elongation in ruminants: roles of progesterone, prostaglandin, interferon tau and cortisol. *J. Anim. Sci. Biotechnol.* **5**, 1–12 (2014).
- Hue, I., Degrelle, S. A. & Turenne, N. Conceptus elongation in cattle: genes, models and questions. *Anim. Reprod. Sci.* **134**, 19–28 (2012).
- Simintiras, C. A. et al. Conceptus metabolomic profiling reveals stage-specific phenotypes leading up to pregnancy recognition in cattle. *Biol. Reprod.* <https://doi.org/10.1093/biolre/iaab021> (2021).
- Degrelle, S. A. et al. Molecular evidence for a critical period in mural trophoblast development in bovine blastocysts. *Dev. Biol.* **288**, 448–460 (2005).
- Mamo, S. et al. RNA sequencing reveals novel gene clusters in bovine conceptuses associated with maternal recognition of pregnancy and implantation. *Biol. Reprod.* **85**, 1143–1151 (2011).
- Ribeiro, E. S. et al. Biology of preimplantation conceptus at the onset of elongation in dairy cows. *Biol. Reprod.* **94**, 1–18 (2016).
- Barnwell, C. V. et al. Differences in mRNA populations of short and long bovine conceptuses on Day 15 of gestation. *Mol. Reprod. Dev.* **83**, 424–441 (2016).
- Simintiras, C. A., Sánchez, J. M., McDonald, M. & Lonergan, P. The biochemistry surrounding bovine conceptus elongation. *Biol. Reprod.* **101**, 328–337 (2019).
- Forde, N. et al. Proteomic analysis of uterine fluid during the pre-implantation period of pregnancy in cattle. *Reproduction* **147**, 575–587 (2014).
- Moraes, J. G. N. et al. Analysis of the uterine lumen in fertility-classified heifers: II. Proteins and metabolites. *Biol. Reprod.* **102**, 571–587 (2020).
- DeSouza, L. et al. Proteomic analysis of the proliferative and secretory phases of the human endometrium: protein identification and differential protein expression. *Proteomics* **5**, 270–281 (2005).
- Simintiras, C. A. et al. Biochemical characterization of progesterone-induced alterations in bovine uterine fluid amino acid and carbohydrate composition during the conceptus elongation window. *Biol. Reprod.* **100**, 672–685 (2019).
- Yan, J., Kuzhiumparambil, U., Bandodkar, S., Dale, R. C. & Fu, S. Cerebrospinal fluid metabolomics: detection of neuroinflammation in human central nervous system disease. *Clin. Transl. Immunol.* **10** (2021).
- Forde, N., Bazer, F. W., Spencer, T. E. & Lonergan, P. 'Conceptualizing' the endometrium: identification of conceptus-derived proteins during early pregnancy in cattle. *Biol. Reprod.* **92**, 1–13 (2015).
- Velazquez, M. A. et al. Sampling techniques for oviductal and uterine luminal fluid in cattle. *Theriogenology* **73**, 758–767 (2010).
- Milo, R. What is the total number of protein molecules per cell volume? A call to rethink some published values. *BioEssays* **35**, 1050–1055 (2013).
- Saumande, J. & Humblot, P. The variability in the interval between estrus and ovulation in cattle and its determinants. *Anim. Reprod. Sci.* **85**, 171–182 (2005).
- Campbell, K. R. & Yau, C. Uncovering pseudotemporal trajectories with covariates from single cell and bulk expression data. *Nat. Commun.* **9**, 2442 (2018).

29. Leese, H. J. et al. Female reproductive tract fluids: composition, mechanism of formation and potential role in the developmental origins of health and disease. *Reprod. Fertil. Dev.* **20**, 1–8 (2008).
30. Levite, M. Response to Comment on “TCR Activation Eliminates Glutamate Receptor GluR3 from the Cell Surface of Normal Human T Cells, via an Autocrine/Paracrine Granzyme B-Mediated Proteolytic Cleavage.” *J. Immunol.* **180**, 2007 (2008).
31. Fang, M. et al. Thermal degradation of small molecules: a global metabolomic investigation. *Anal. Chem.* **87**, 10935–10941 (2015).
32. Rabaglino, M. B. et al. Application of one injection of prostaglandin F(2alpha) in the five-day Co-Synch+CIDR protocol for estrous synchronization and resynchronization of dairy heifers. *J. Dairy Sci.* **93**, 1050–1058 (2010).
33. Sartori, R. et al. Improvement in recovery of embryos/ova using a shallow uterine horn flushing technique in superovulated Holstein heifers. *Theriogenology* **60**, 1319–1330 (2003).
34. Pohler, K. G. et al. Circulating concentrations of bovine pregnancy-associated glycoproteins and late embryonic mortality in lactating dairy herds. *J. Dairy Sci.* **99**, 1584–1594 (2016).
35. Simintiras, C. A. et al. Capture and metabolomic analysis of the human endometrial epithelial organoid secretome. *Proc. Natl Acad. Sci. USA* **118**, e2026804118 <https://doi.org/10.1073/pnas.2026804118> (2021).
36. Wolf, F. A. et al. PAGA: graph abstraction reconciles clustering with trajectory inference through a topology preserving map of single cells. *Genome Biol.* **20**, 59 (2019).
37. Hammer, Ø., Harper, D. A. T. & Ryan, P. D. PAST: paleontological statistics software package for education and data analysis. *Palaeontol. Electron.* **4**, 1–9 (2001).
38. Simintiras, C. A. et al. Uterine lumen fluid is metabolically semi-autonomous. *Dryad* <https://doi.org/10.5061/dryad.sbcc2fr7t> (2022).

Acknowledgements

We appreciate Dr. Michael F. Smith for performing the progesterone radioimmunoassay. This work was supported by the Eunice Kennedy Shriver National Institute of Child Health and Development (NIH R01 HD096266), a Tier 2 award from the University of Missouri System Research and Creative Works Strategic Investment Program, and a USDA-AFRI Competitive Grant (2019-67015-28998).

Author contributions

C.A.S. and T.E.S. conceived the project and designed the experiments. C.A.S., J.N.D., and M.S.O. performed the research. C.A.S. and H.L. analyzed the data. C.A.S. and T.E.S. wrote the paper. All authors approved this submission.

Competing interests

The authors declare no competing interests.

Additional information

Supplementary information The online version contains supplementary material available at <https://doi.org/10.1038/s42003-022-03134-0>.

Correspondence and requests for materials should be addressed to Thomas E. Spencer.

Peer review information *Communications Biology* thanks the anonymous reviewers for their contribution to the peer review of this work. Primary Handling Editors: Christopher Hine and Caitlin Karniski.

Reprints and permission information is available at <http://www.nature.com/reprints>

Publisher's note Springer Nature remains neutral with regard to jurisdictional claims in published maps and institutional affiliations.



Open Access This article is licensed under a Creative Commons Attribution 4.0 International License, which permits use, sharing, adaptation, distribution and reproduction in any medium or format, as long as you give appropriate credit to the original author(s) and the source, provide a link to the Creative Commons license, and indicate if changes were made. The images or other third party material in this article are included in the article's Creative Commons license, unless indicated otherwise in a credit line to the material. If material is not included in the article's Creative Commons license and your intended use is not permitted by statutory regulation or exceeds the permitted use, you will need to obtain permission directly from the copyright holder. To view a copy of this license, visit <http://creativecommons.org/licenses/by/4.0/>.

© The Author(s) 2022